ISSN 1674-1056
http://cpb.iphy.ac.cn
http://iopscience.iop.org/cpb
中国物理 B
Chinese Physics
中国物理 Chinese Physics B

Simulation and experimental study of a novel bifacial structure of silicon heterojunction solar cell for high efficiency and low cost

Haibin Huang(黄海宾), Gangyu Tian(田罡煜), Lang Zhou(周浪), Jiren Yuan(袁吉仁), Wolfgang R. Fahrner, Wenbin Zhang(张闻斌), Xingbing Li(李杏兵), Wenhao Chen(陈文浩), Renzhong Liu(刘仁中)
Citation: Chin. Phys. B . 2018, 27(3): 038502. **doi:** 10.1088/1674-1056/27/3/038502

Journal homepage: http://cpb.iphy.ac.cn; http://iopscience.iop.org/cpb

What follows is a list of articles you may be interested in

Effects of proton irradiation at different incident angles on InAlAs/InGaAs InP-based HEMTs

Shu-Xiang Sun(孙树祥), Zhi-Chao Wei(魏志超), Peng-Hui Xia(夏鹏辉), Wen-Bin Wang(王文斌), Zhi-Yong Duan(段智勇), Yu-Xiao Li(李玉晓), Ying-Hui Zhong(钟英辉), Peng Ding(丁芃), Zhi Jin(金智)
Chin. Phys. B . 2018, 27(2): 028502. **doi:** 10.1088/1674-1056/27/2/028502

Detailed study of NBTI characterization in 40-nm CMOS process using comprehensive models

Yan Zeng(曾严), Xiao-Jin Li(李小进), Jian Qing(卿健), Ya-Bin Sun(孙亚宾), Yan-Ling Shi(石艳玲), Ao Guo(郭奥), Shao-Jian Hu(胡少坚)
Chin. Phys. B . 2017, 26(10): 108503. **doi:** 10.1088/1674-1056/26/10/108503

Improved high-frequency equivalent circuit model based on distributed effects for SiGe HBTs with CBE layout

Ya-Bin Sun(孙亚宾), Xiao-Jin Li(李小进), Jin-Zhong Zhang(张金中), Yan-Ling Shi(石艳玲)
Chin. Phys. B . 2017, 26(9): 098502. **doi:** 10.1088/1674-1056/26/9/098502

Impact of energy straggle on proton-induced single event upset test in a 65-nm SRAM cell

Bing Ye(叶兵), Jie Liu(刘杰), Tie-Shan Wang(王铁山), Tian-Qi Liu(刘天奇), Jie Luo(罗捷), Bin Wang(王斌), Ya-Nan Yin(殷亚楠), Qing-Gang Ji(姬庆刚), Pei-Pei Hu(胡培培), You-Mei Sun(孙友梅), Ming-Dong Hou(侯明东)
Chin. Phys. B . 2017, 26(8): 088501. **doi:** 10.1088/1674-1056/26/8/088501

An optimized fitting function with least square approximation inInAs/AlSb HFET small-signal model for characterizingthe frequency dependency of impact ionization effect

He Guan(关赫), Hui Guo(郭辉)
Chin. Phys. B . 2017, 26(5): 058501. **doi:** 10.1088/1674-1056/26/5/058501

Simulation and experimental study of a novel bifacial structure of silicon heterojunction solar cell for high efficiency and low cost*

Haibin Huang(黄海宾)[1], Gangyu Tian(田罡煜)[1], Lang Zhou(周浪)[1,†], Jiren Yuan(袁吉仁)[1,2,‡], Wolfgang R. Fahrner[1], Wenbin Zhang(张闻斌)[3], Xingbing Li(李杏兵)[3], Wenhao Chen(陈文浩)[4], and Renzhong Liu(刘仁中)[4]

[1] *Institute of Photovoltaics, Nanchang University, Nanchang* 330031, *China*
[2] *Department of Physics, Nanchang University, Nanchang* 330031, *China*
[3] *GCL System Integration Technology Co. Ltd., Shanghai* 201700, *China*
[4] *Hareon Solar Co. Ltd., Taicang* 215400, *China*

(Received 6 December 2017; revised manuscript received 25 December 2017; published online 13 February 2018)

A novel structure of Ag grid/SiN_x/n^+-c-Si/n-c-Si/i-a-Si:H/p^+-a-Si:H/TCO/Ag grid was designed to increase the efficiency of bifacial amorphous/crystalline silicon-based solar cells and reduce the rear material consumption and production cost. The simulation results show that the new structure obtains higher efficiency compared with the typical bifacial amorphous/crystalline silicon-based solar cell because of an increase in the short-circuit current (J_{sc}), while retaining the advantages of a high open-circuit voltage, low temperature coefficient, and good weak-light performance. Moreover, real cells composed of the novel structure with dimensions of 75 mm × 75 mm were fabricated by a special fabrication recipe based on industrial processes. Without parameter optimization, the cell efficiency reached 21.1% with the J_{sc} of 41.7 mA/cm^2. In addition, the novel structure attained 28.55% potential conversion efficiency under an illumination of AM 1.5 G, 100 mW/cm^2. We conclude that the configuration of the Ag grid/SiN_x/n^+-c-Si/n-c-Si/i-a-Si:H/p^+-a-Si:H/TCO/Ag grid is a promising structure for high efficiency and low cost.

Keywords: silicon solar cell, a-Si:H/c-Si heterojunction, short-circuit current

PACS: 85.30.De, 88.30.gg, 85.60.Gz **DOI:** 10.1088/1674-1056/27/3/038502

1. Introduction

In past years, hydrogenated amorphous/crystalline silicon (a-Si:H/c-Si)-based heterojunction solar cells have been intensively investigated because of their high open-circuit voltage (V_{oc}), low temperature coefficient, and bifacial power generation.[1–10] This a-Si:H/c-Si heterojunction solar cell is called heterojunction with intrinsic thin film (HIT) photovoltaic device and had a conversion efficiency of 18.1% in 1992. Recently, the HIT solar cell with interdigitated back contact (IBC) technology has achieved a world-record efficiency of over 26%.[11,12] For HIT solar cells, the optical absorption loss at the illumined front of the cell is a critical issue because a-Si:H possesses a very high absorption coefficient. Holman *et al.*[13] proposed that a relative efficiency increase of over 5% is possible for the HIT solar cell if the optical absorption loss can be reduced. For this purpose, materials with low absorption coefficients and wide bandgaps were proposed to replace a-Si:H as the emitter of the HIT solar cell.[14–16] IBC technology was introduced to the HIT solar cell to reduce the optical absorption loss by placing the emitter of the a-Si:H layer and the grid electrodes at the back side of the cell.[11,12] However, the IBC structure is complicated and difficult to fabricate for mass production. Here, to maintain the advantage of bifacial power generation and reduce the optical absorption loss, a novel silicon heterojunction structure of Ag grid/SiN_x/n^+-c-Si/n-c-Si/i-a-Si:H/p^+-a-Si:H/TCO/Ag grid (HAC cell) was designed, and its fabrication recipe based on an industrial process is proposed. The design structure and proposed fabrication recipe have the following advantages: (i) the optical absorption loss at the illumined front of the cell is greatly reduced, (ii) the series resistance is reduced by replacing the low-temperature solidified Ag grids with high-temperature-fired Ag grids and removing the intrinsic high-resistivity a-Si:H layer; (iii) the expensive ITO materials accounting for about 10% of the cost of the raw materials for a piece of HIT cell can be reduced by 50%, and (iv) the fabrication processes are compatible with normal homojunction c-Si production lines, and the investment cost of a new HAC solar cell production line can be very economical because of the special fabrication recipe design. In this work, the performance of the HAC cells was studied and compared with that of the HIT cells by numerical simulation. The HAC cells were fabricated according to the proposed recipe with feasible industrial technologies. The characterization of the HAC cells is analyzed and discussed.

*Project supported by the Jiangxi Provincial Key Research and Development Foundation, China (Grant No. 2016BBH80043), the Open Fund of Jiangsu Key Laboratory of Materials and Technology for Energy Conversion, China (Grant No. NJ20160032), and the National Natural Science Foundation of China (Grant Nos. 61741404, 61464007, and 51561022).

†Corresponding author. E-mail: lzhou@ncu.edu.cn
‡Corresponding author. E-mail: yuanjiren@ncu.edu.cn

© 2018 Chinese Physical Society and IOP Publishing Ltd

2. Simulation and experiment

2.1. Simulation methodology

The wxAMPS program[17,18] was used for the solar cell simulation. The simulation principle was based on the Poisson equation and the hole and electron continuity equations. Figure 1 illustrates the schematic structure of the HIT and HAC solar cells used in this study. Figures 1(a) and 1(b) show typical HIT solar cell structures, and their difference is the incident side of light, i.e., the light is incident from the p-a-Si:H side in Fig. 1(a) and from the n-a-Si:H side in Fig. 1(b). Figures 1(c) and 1(d) have the same structure of the HAC solar cell, but the incident side of light is reversed. Note that the sunlight is mainly incident from the top side of the cell, and some sunlight can be reflected to the bottom side. For convenience, the sunlight reflected to the bottom side of the cell was not taken into consideration in this work because of its weak intensity. The material parameters[15,19] are shown in Table 1.

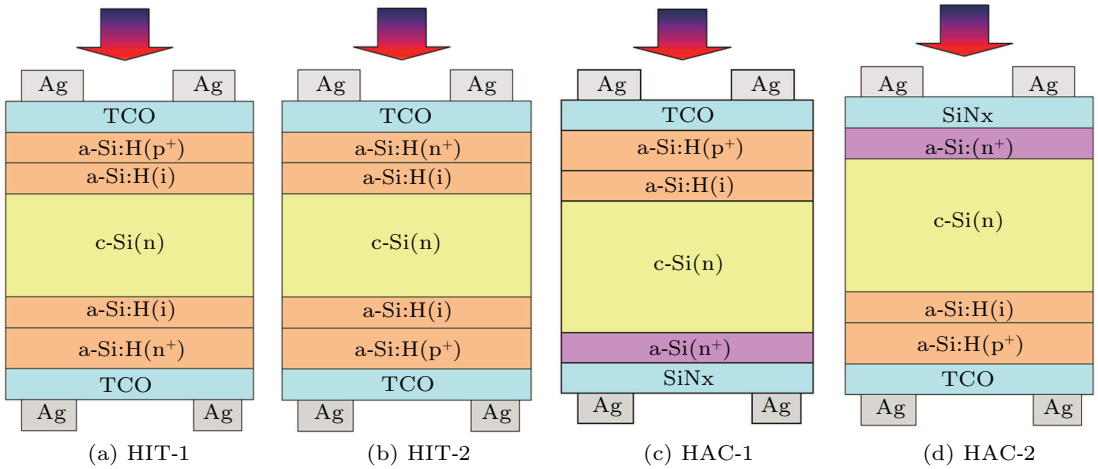


Fig. 1. (color online) Schematic of silicon heterojunction solar cells with different structures: (a) HIT-1, (b) HIT-2, (c) HAC-1, and (d) HAC-2.

Table 1. Main simulation parameters of HIT and HAC solar cells.

Parameter and unit	a-Si:H(p$^+$)	a-Si:H(i)	a-Si:H(n)	c-Si(n)	c-Si(n$^+$)
Thickness/nm	10	5	10	variable	5×10^3
Electron affinity/eV	3.80	3.80	3.80	4.05	4.05
Band gap/eV	1.72	1.72	1.72	1.12	1.12
Relative dielectric constant	11.90	11.90	11.90	11.90	11.90
Effective conduction band density/cm^{-3}	2.50×10^{20}	2.50×10^{20}	2.50×10^{20}	2.80×10^{19}	2.80×10^{19}
Effective valence band density/cm^{-3}	2.50×10^{20}	2.50×10^{20}	2.50×10^{20}	1.04×10^{19}	1.04×10^{19}
Electron mobility/cm$^2\cdot$V$^{-1}\cdot$s^{-1}	10	20	10	1350	1350
Hole mobility/cm$^2\cdot$V$^{-1}\cdot$s^{-1}	2	5	2	450	450
Donor concentration/cm^{-3}	0	0	1×10^{19}	3×10^{15}	1×10^{18}
Acceptor concentration/cm^{-3}	6×10^{18}	0	0	0	0
Band tail density of states/cm$^{-3}\cdot$eV^{-1}	1×10^{21}	1×10^{21}	1×10^{21}	1×10^{14}	1×10^{14}
Characteristic energy for donors, acceptors/eV	0.04, 0.06	0.04, 0.06	0.04, 0.06	0.01, 0.01	0.01, 0.01
Capture cross-section for donor states, e, h[a] (cm^2)-Band tails	1×10^{-15}, 1×10^{-17}	1×10^{-15}, 1×10^{-17}	1×10^{-15}, 1×10^{-17}	1×10^{-15}, 1×10^{-17}	1×10^{-15}, 1×10^{-17}
Capture cross-section for acceptor states, e, h (cm^2)-Band tails	1×10^{-17}, 1×10^{-15}	1×10^{-17}, 1×10^{-15}	1×10^{-17}, 1×10^{-15}	1×10^{-17}, 1×10^{-15}	1×10^{-17}, 1×10^{-15}
Gaussian density of states/cm^{-3}	7×10^{18}, 7×10^{18}	5×10^{16}, 5×10^{16}	1×10^{18}, 1×10^{18}	–	–
Gaussian peak energy for donors, acceptor/eV	1.22, 1.22	1.22, 1.22	1.22, 1.22	–	–
Standard deviation/eV	0.08	0.08	0.08	–	–
Capture cross-section for donor states, e, h (cm^2)-Midgap	1×10^{-14}, 1×10^{-15}	1×10^{-14}, 1×10^{-15}	1×10^{-14}, 1×10^{-15}	–	–
Capture cross-section for acceptor states, e, h (cm^2)-Midgap	1×10^{-15}, 1×10^{-14}	1×10^{-15}, 1×10^{-14}	1×10^{-15}, 1×10^{-14}	–	–
Midgap density of states in c-Si/cm$^{-3}\cdot$eV^{-1}	–	–	–	1×10^{12}	1×10^{12}
Switch-over energy/eV	–	–	–	0.56	0.56
Capture cross-section for donor states, e, h/cm^2	–	–	–	1×10^{-14}, 1×10^{-15}	1×10^{-14}, 1×10^{-15}
Capture cross-section for acceptor states, e, h/cm^2	–	–	–	1×10^{-15}, 1×10^{-14}	1×10^{-15}, 1×10^{-14}

[a] e, h represents the electron and hole, respectively.

The surface recombination velocities of electrons and holes at the front and back contact interface were both set to 10^7 cm/s. The simulated condition was under AM 1.5 G, 100 mW/cm^2, and 300 K.

2.2. Experiment details

The schematic of the fabricated HAC cells is shown in Fig. 2(a). Figure 2(b) shows the processing recipe for the HAC cells. A sample of the 75-nm × 75-mm HAC cell is shown in Fig. 2(c). The cells were prepared with a normal n-type solar-grade single crystalline-silicon wafer, (100) orientation, 180 μm, 2–5 Ω·cm. The wafer was textured by KOH solutions and rounded by HNO_3/HF mixed solutions, then cleaned with RCA solutions, dipped in HF, and dried by N_2. Approximately 20 μm of Si was etched on each side. During the process, the top illumined side of the cell was made first and needed higher temperatures than the other side. All steps were performed on a normal production line (Hareon Solar Co. Ltd.) for c-Si solar cells. In the "cleaning III" step, only the naked side of the wafer was cleaned, while the finished side of the wafer was protected. The naked side of the wafer was cleaned by HF, an HNO_3/HF mixed solution, SC1, SC2, and HF in sequence. The intrinsic and p-type a-Si:H layers were made by PECVD (13.56 MHz), and the ITO layer was deposited by the reactive plasma deposition method. The Ag grids on the ITO layer were made by screen printing with a low-temperature Ag paste and were solidified at 220 °C. After the cell was fabricated, it was cut into 75-nm × 75-mm pieces by laser for uniformity.

Current–voltage curves of the cells were tested (AM 1.5 G, 25 °C) with light injected from the top side and bottom side separately. The external and internal quantum efficiencies (EQE and IQE) were measured by QE-R3018 (Guang Yan, Taiwan, China). The resistances of the same-length fired Ag grids and the solidified Ag grid on both sides of the cell were tested with a current–voltage tester.

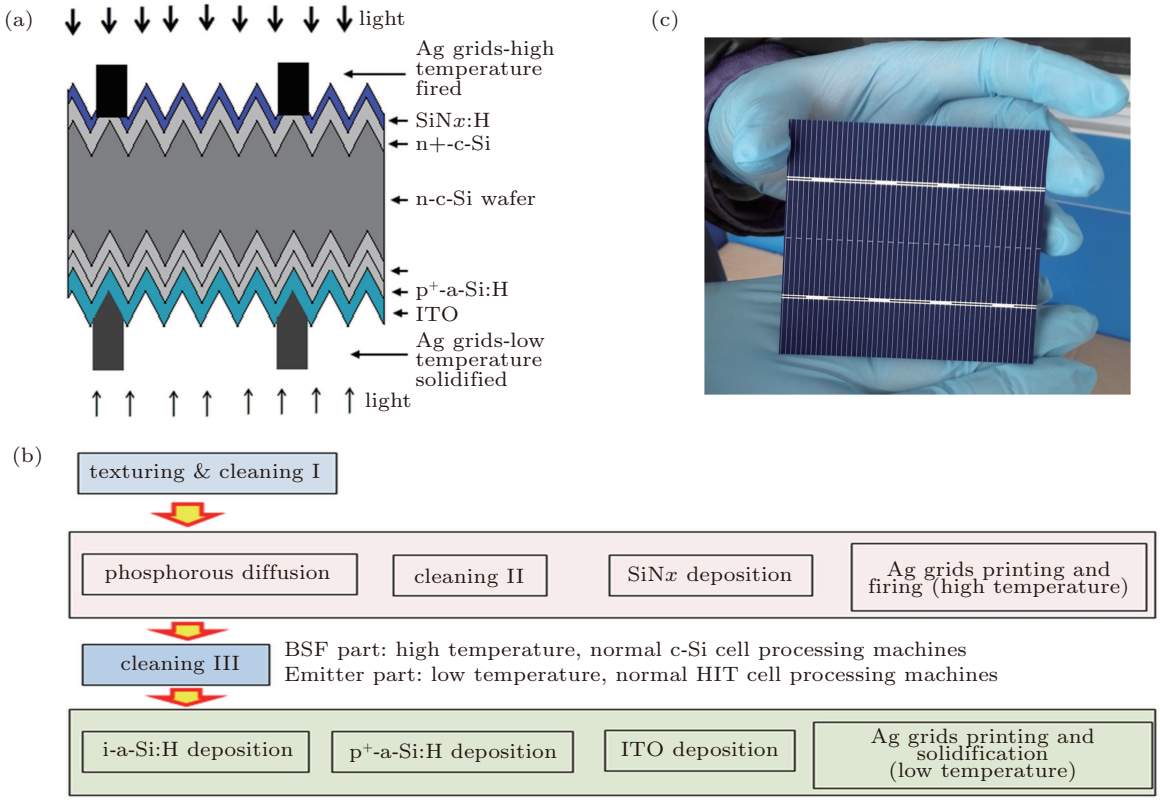


Fig. 2. (color online) Processing recipe and profile of fabricated bifacial HAC cells: (a) schematic of HAC cell, (b) processing recipe for HAC cell, and (c) sample of 75-nm × 75-mm HAC cell.

3. Results and discussion

Figure 3 shows the simulation results of the HIT and HAC cells with different wafer thicknesses. It was found that the HAC cell with the light injected from the SiN_x side had the best efficiency for different wafer thicknesses, while the HIT-2 cell had the worst performance. The efficiencies of the HIT-1 and HAC-1 cells were nearly identical when the wafer thicknesses were the same. From the simulation result of the short-circuit current, open-circuit voltage, and fill factor (FF), it is clear that the efficiency gain of the HAC-2 cell was a result of an increase in J_{sc}. The current increase occurred as a result of the reduction of the parasitic absorption loss because the structure of the HAC-2 cell employs n^+-c-Si layer as the emitter, whereas other cells use n^+-a-Si:H or p^+-a-Si:H layers

as emitters. It is well known that a-Si:H materials have a very high absorption coefficient and very low mobility. Therefore, the collection efficiency of photocarriers in the a-Si:H emitter of the HAC-1 cell is very low. In other words, the photons absorbed by an a-Si:H layer are hardly used and are wasted. The QE curves of the cell in Fig. 3(e) indicate that little absorption loss was found in the short-wavelength region of the HAC-2 cell. It can be seen from Fig. 3(c) that the V_{oc}s of the HAC and HIT cells had no obvious differences, meaning that the HAC cell maintained the high V_{oc} feature of the a-Si:H/c-Si structure. For the reverse saturation currents (J_0s) of the HAC and HIT cells, it is observed from Fig. 3(f) that the gaps of J_0s between the HAC and HIT cells was small and that the HAC cells retained the low temperature coefficient and good weak-light performance of the a-Si:H/c-Si structure.[20]

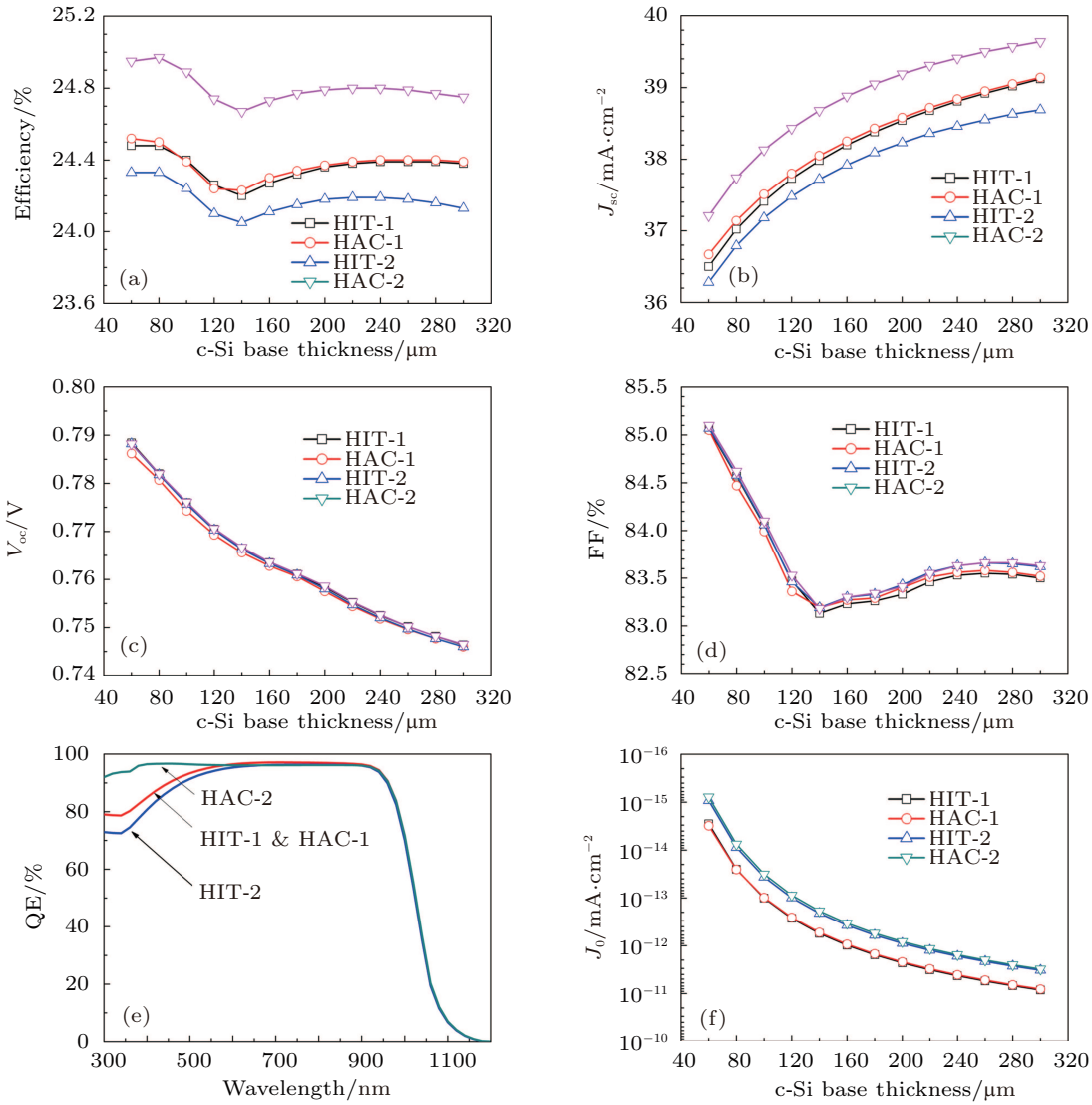


Fig. 3. (color online) Simulation results of HAC and HIT cells with different wafer thicknesses: (a) variation of conversion efficiency with wafer thickness, (b) variation of short-circuit current density with wafer thickness, (c) variation of open-circuit voltage V_{oc} with wafer thickness, (d) variation of fill factor FF with wafer thickness, (f) quantum efficiency *QE* as a function of wavelength, and (e) reverse saturation currents J_0s with different wafer thicknesses.

Figure 4 shows the resistance testing result of the high-temperature-fired Ag grids and the low-temperature solidified Ag grids for the HAC cell. The resistance of the high-temperature-fired Ag grids was 0.16 Ω and that of the low-temperature solidified grid was 0.23 Ω. The new design reduced the resistance of the grids.

Figure 5 shows the EQE and IQE of the fabricated HAC cells. The blue light response was significantly improved for the HAC-2 cell, while a large absorption loss in the short-wavelength region was clearly observed for the HAC-1 cell. The results agree well with the simulated curves in Fig. 3(e) because the a-Si:H layer used as an emitter absorbed many photons in the ultraviolet region which could not then contribute to the current for the HAC-1 cell. Moreover, the bandgap of SiN_x is higher than that of the ITO layer, therefore, many photons in the ultraviolet region passed through

the SiN_x layer and were usefully absorbed. Therefore, the SiN_x film/n^+-c-Si structure is better than the ITO/n^+-a-Si:H/i-a-Si:H structure. It should be noted that although the glass used to encapsulate the cells had strong absorption in the UV region, its absorption waveband was about 280–320 nm.[21] In this waveband, the photon flux of sunlight is very small, therefore, the encapsulated glass had little impact on the performance of the cells.

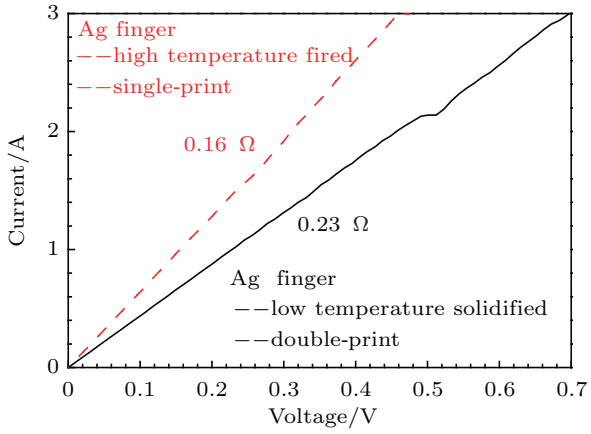


Fig. 4. (color online) Resistances of high-temperature-fired Ag grid and low-temperature-solidified Ag grid for the HAC cell tested by dark current-voltage measurement.

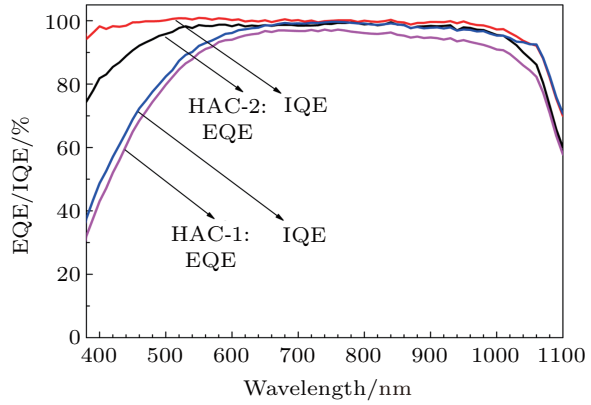


Fig. 5. (color online) EQE and IQE curves of HAC cells fabricated based on industrial processes.

The performance of the sample prepared with the recipe shown in Fig. 2(b) is shown in Fig. 6. It can be seen that the J_{sc}s of the HAC-1 and HAC-2 reached 38.7 mA/cm^2 and 41.7 mA/cm^2, respectively, and the values of V_{oc} and FF were not good. The conversion efficiencies of the HAC-1 and HAC-2 were 19.1% and 21.1%, respectively. Although the efficiency of the HAC cell in the laboratory was lower than the world's highest conversion efficiency, the performance of the HAC cells was obtained with existing production lines (Hareon Solar Co. Ltd.), and no processing parameters were optimized. The V_{oc} and FF could have been improved if the processing parameters had been further optimized. Moreover, the uncomplicated structure of the HAC cells, compared to that of an IBC-type cell, facilitates mass production. In addition, the new structure reduces fabrication costs because of the 50% savings on the amount ITO material required, the use of less costly machines, and its compatibility with the conventional c-Si solar cell production line.

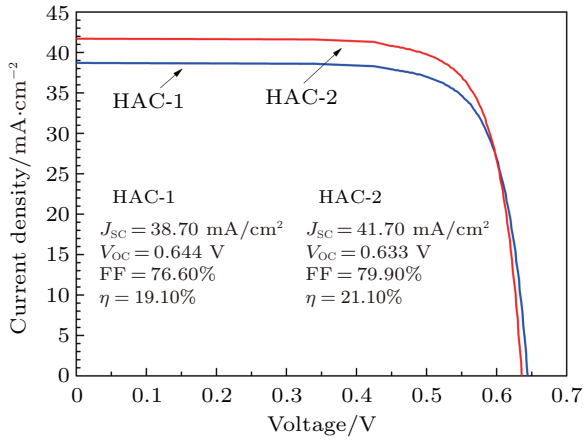


Fig. 6. (color online) Performance of HAC cells fabricated based on industrial processes.

The HAC cell is a promising structure in light of the primary experiment results. To evaluate the potential conversion efficiency for these HAC and HIT cells the wxAMPS program was employed to calculate the potential performance by optimizing device parameters. As shown in Fig. 7, the potential conversion efficiency of the HAC cell attained 28.55% under illumination of AM 1.5 G, 100 mW/cm^2, while that of the HIT cell was 27.06% under the same conditions This indicates that the HAC cell obtained a higher efficiency than the HIT cell.

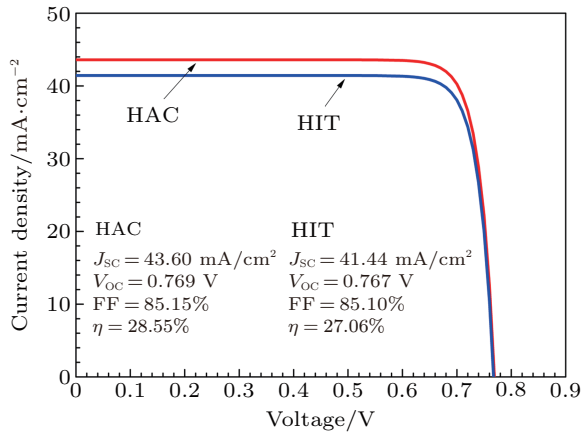


Fig. 7. (color online) Potential performance of HAC and HIT cells.

4. Conclusions

A novel structure of Ag grid/SiN_x/n^+-c-Si/n-c-Si/i-a-Si:H/p^+-a-Si:H/TCO/Ag grid was designed to increase the efficiency of a-Si:H/c-Si-based solar cells and reduce fabrication costs. According to our simulation results, the new structure increased the efficiency of a-Si:H/c-Si-based solar cells by increasing J_{sc} and retaining most of the advantages of an HIT

cell. Moreover, according to our proposed fabrication recipe based on industrial processes without parameter optimization, an HAC cell with dimensions 75 mm × 75 mm was successfully fabricated with an efficiency of 21.1% and a J_{sc} of 41.7 mA/cm^2. In addition, a conversion efficiency of 28.55% could be obtained for an optimized HAC cell. The results show that the novel HAC cell structure has great potential for high efficiency and low-cost fabrication.

Acknowledgements

The authors acknowledge Mr. Hong Wang from Ideal Deposition Equipment and Applications (Shanghai) Ltd. for his assistance in the sample preparation.

References

[1] Tanaka M, Taguchi M, Matsuyama T, Sawada T, Tsuda S, Nakano S, Hanafusa H and Kuwano Y 1992 *Jpn. J. Appl. Phys.* **31** 3518
[2] Taguchi M, Kawamoto K, Tsuge S, Baba T, Sakata H, Morizane M, Uchihashi K, Nakamura N, Kiyama S and Oota O 2000 *Prog. Photovolt: Res. Appl.* **8** 503
[3] Tsunomura Y, Yoshimine Y, Taguchi M, Baba T, Kinoshita T, Kanno H, Sakata H, Maruyama E and Tanaka M 2009 *Sol. Energy Mater. Sol. Cells* **93** 670
[4] Datta A, Rahmouni M, Nath M, Boubekri R, Cabarrocas P R and Chatterjee P 2010 *Sol. Energy Mater. Sol. Cells* **94** 1457
[5] Taguchi M, Yano A, Tohoda S, Matsuyama K, Nakamura Y, Nishiwaki T, Fujita K and Maruyama E 2014 *IEEE J. Photovolt.* **4** 96
[6] Adachi D, Hernandez J L and Yamamoto K 2015 *Appl. Phys. Lett.* **107** 233506
[7] Gu J H, Si J L, Wang J X, Feng Y Y, Gao X Y and Lu J X 2015 *Chin. Phys. B* **24** 117703
[8] Meng F, Liu J, Shen L, Shi J, Han A, Zhang L, Liu Y, Yu J, Zhang J, Zhou R and Liu Z 2017 *Front. Energy* **11** 78
[9] Bashiri H, Karami M A and Mohammadnejad S 2017 *Chin. Phys. B* **26** 108801
[10] Liu W, Zhang L, Cong S, Chen R, Wu Z, Meng F, Shi Q and Liu Z 2018 *Sol. Energy Mate. Sol. Cells* **174** 233
[11] Yoshikawa K, Kawasaki H, Yoshida W, Irie T, Konishi K, Nakano K, Uto T, Adachi D, Kanematsu M, Uzu H and Yamamoto K 2017 *Nat. Energy* **2** 17032
[12] Yoshikawa K, Yoshida W, Irie T, Kawasaki H, Konishi K, Ishibashi H, Asatani T, Adachi D, Kanematsu M, Uzu H and Yamamoto K 2017 *Sol. Energy Mater. Sol. Cells* **173** 37
[13] Holman Z C, Descoeudres A, Barraud L, Fernandez F Z, Seif J P, Wolf S D and Ballif C 2012 *IEEE J. Photovolt.* **2** 7
[14] He Y, Huang H, Zhou L, Yue Z, Yuan J, Zhou N and Gao C 2017 *Mater. Sci. Semicond. Process.* **6** 1
[15] Yuan J, Shen H, Lu L, Wu T and He X 2010 *Optoelectron. Adv. Mater. Rapid Commun.* **4** 1211
[16] Kirner S, Mazzarella L, Korte L, Stannowski B, Rech B and Schlatmann R 2015 *IEEE J. Photovolt.* **5** 1601
[17] Liu Y, Sun Y and Rockett A 2012 *Sol. Energy Mater. Sol. Cells* **98** 124
[18] Zhu H, Kalkan A K, Hou J and Fonash S J 1999 *AIP Conf. Proc.* **462** 309
[19] Hernández-Como N and Morales-Acevedo A 2010 *Sol. Energy Mater. Sol. Cells* **94** 62
[20] Tauchi M, Terakawa A, Maruyama E and Tanaka M 2005 *Prog. Photovol.: Res. Appl.* **13** 481
[21] Wang C Y and Tao Y 2003 *Glass Enamel* **31** 59